

# *A Simple Method to Evaluate Structural Stability of Group IV and III-V Semiconductors*

Shigetoshi NARA<sup>1</sup>, Shigeru MIHO and Hiroo TOTSUJI<sup>1</sup>

(Received September 30 , 1993)

## SYNOPSIS

The structural stabilities of bulk Si, Ge, and GaAs are discussed based on the total energy evaluated by the summation of the band structure energy and the short-range repulsive potential between ions. The band structure energy is calculated by means of the simple tight-binding method. The tight-binding parameters are determined so as to fit to the results of a pseudopotential calculation and Harrison's model is employed to include the influence of lattice deformation. The short-range-force is assumed to be of the exponential form and parameters are determined so as to reproduce an experimental value of bulk modulus. This treatment qualitatively well describes structural properties in spite of the simple computational procedure and roughly gives the known variation of the total energy for a  $\langle 100 \rangle$  uniaxial strain. This method is able to be applied to an investigation of the structural stabilities of superlattices, for example, a strained layer superlattice consisting of hetero-semiconductors.

---

<sup>1</sup>Department of Electrical and Electronic Engineering

## 1 Introduction

Nowadays it is important to develop semiconductor material technologies which enable us to have tailorable electronic or optical properties. Semiconductors are extensively investigated not only to develop a novel device but also related with the above mentioned viewpoint. Owing to the great development of thin film crystal growth technologies which enable us to control in a scale of monoatomic layer, for example, using MBE [1] (molecular-beam epitaxy) and MOCVD [1] (metal organic chemical vapor deposition), a large number of artificial crystal structures are made, for instance, such as superlattices.

Before such experimental trial is done, it is meaningful if one can theoretically evaluate expected structural or electronic properties of artificially designed crystalline materials using those of each individual properties. Although a theoretical treatment based on the computational physics describing the properties of material have been significantly improved, an accurate prediction about the properties of hypothetical materials are still difficult because of numerical complexity and waste of computer time. It is our motivation that we propose a simple approximative method to describe total energies of bulk semiconductors and apply it to an evaluation of structural stability of superlattices, while the accuracy is lost a little with respect to the predictability of structural and electronic properties of hypothetical materials.

Generally speaking, in order to study the structural stability of a material, it is necessary to discuss a variation of total energy as a function of lattice deformations. Therefore hopefully an accurate estimation of the total energy is requested. It is well known that the total energy of condensed matters consist of two contributions which are an attractive energy originated from electronic state and repulsive energy between ion cores, respectively.

In this paper we discuss the total energy with including of the dependence on lattice deformations by evaluating the summation of the band structure energy and the short-range repulsive potential between ion cores.

In §2, we give a brief description of crystal structures of semiconductor, and give our procedure of the total energy calculations.

In §3, we calculate the electronic energy band structures for bulk Si, Ge, and GaAs by means of the simple Tight-Binding (TB) method [2] which reproduces the results of Empirical Pseudo-potential Method ( EPM ) [3]. In order to determine the band parameters under the existence of strain, we use Harrison's model.

In section 4, we calculate the repulsive part based on a short-range-force model assuming an exponential form of repulsive potential including two parameters.

In section 5, this method is applied to the case of deformed lattice obtained uniform contraction or expansion and is extended to the case under the existence of a  $\langle 100 \rangle$  uniaxial strain.

## 2 Crystal Structures

### 2.1 Diamond and Zincblende Structures

The group IV and III-V semiconductors, Si, Ge, GaAs and so on, have the diamond or zincblende structure [4]. In the diamond structure typically observed in the group IV semiconductor, each atom is tetrahedrally bonded with four nearest neighbors. And there are two atoms in the unit cell. This structure is consisting of two interpenetrating face-centered cubic ( f.c.c. ) Bravais lattice displaced along the body diagonal direction with  $(a/4, a/4, a/4)$ , where  $a$  is the lattice constant.

The zincblende structure typically observed in the group III-V or II-VI compounds is closely related to that of diamond structure. It can be given from a diamond lattice by putting cation atoms on one sublattice and anion atoms on the other sublattice. The schematical illustration of the zincblende structure is shown in fig.1. The first Brillouin zone [4] is shown in fig.2. The high symmetry points  $\Gamma$ ,  $X$ ,  $K$ ,  $U$ , and  $W$  are also plotted.

## 2.2 Structural Stability

Under the existence of lattice deformation, a crystal structure exhibit a change in shape and volume. If a given crystal structure is stable, the total energy must increase when any distortion is externally applied. So it is necessary to evaluate total energies as a function of lattice deformation.

Our aim is to evaluate total energies numerically by a rather simple method without handling the difficult and complicated method of *ab initio* calculation although in such simple method the reliability of results is lost with some extent by the "trade-off" between accuracy and easiness of calculation.

In general, attractive force between atoms are originated from the effect of lowering energies due to the valence electrons. But when atomic distance becomes smaller for the inner shell electrons to contact each other, a large repulsive force due to the Pauli principle between core electrons appears and prevents the atoms from being close any more. Therefore crystal structure is determined with a balance between attractive force and repulsive force.

As noted in the introduction, the total energy  $E_{tot}$  of a present system is approximated as

$$E_{tot} = \{\text{attractive energy}\} + \{\text{repulsive energy}\} . \quad (1)$$

An attractive energy is called an electronic band-structure energy  $E_{bs}$  defined as

$$E_{bs} = \sum_{\mathbf{k}, n} E_n(\mathbf{k}) , \quad (2)$$

where the sum is over occupied single particle states with wave vector  $\mathbf{k}$  and band index  $n$ . Thus,

$$E_{tot} = E_{bs} + U , \quad (3)$$

where  $U$  is a repulsive energy part and is well approximated by a short-range-force model because ions are separated by a distance much larger than the Thomas-Fermi screening length. In the present paper, the variation in  $U$  with atomic displacements is assumed to be described by a exponential type model. This type model gives us a very rapid convergence on the numerical calculation.

Now, numerical calculation for  $E_{bs}$  is given by replacing the eq.(2) with the integral of the density of states  $N(E)$ , and are denoted as

$$E_{bs} = \int_{-\infty}^{E_F} EN(E)dE \quad , \quad (4)$$

where the integration is taken over all occupied states, i.e. all over the valence band, and  $E$  is energy.  $N(E)$  is density of states calculated by a computational treatment as following section 3.

### 3 Energy Band Structure Calculations by Means of a Simple Tight-Binding Method

#### 3.1 Tight-Binding Method

A tight-binding method [2] starts with an atomic orbital  $\phi_n(\mathbf{r} - \mathbf{R}_l)$ , located on an atom at vector position  $\mathbf{R}_l$ .  $n$  specifies one of f.c.c. sublattices  $\alpha$  or  $\beta$  and one of four valence atomic orbitals where their symmetry types are symbolized by  $s$ ,  $p_x$ ,  $p_y$ , and  $p_z$ . Then we can prepare the Bloch wave function as

$$\psi_n(\mathbf{k}, \mathbf{r}) = \sum_l e^{i\mathbf{k}\cdot\mathbf{R}_l} \phi_n(\mathbf{r} - \mathbf{R}_l) \quad , \quad (5)$$

where the summation runs over all atomic site of a f.c.c. sublattice. Using this Bloch wavefunctions, the Hamiltonian matrix elements are defined as

$$E_{n,m} \equiv \int \phi_n^*(\mathbf{r}) \mathcal{H} \phi_m(\mathbf{r} - \mathbf{R}_l) d\mathbf{r} \quad , \quad (6)$$

where  $\mathcal{H}$  is the Hamiltonian operator and a vector  $\mathbf{R}_l$  is

$$\mathbf{R}_l = p\mathbf{i} + q\mathbf{j} + r\mathbf{k} \quad , \quad (7)$$

where  $p$ ,  $q$ ,  $r$  are integer and  $\mathbf{i}$ ,  $\mathbf{j}$ ,  $\mathbf{k}$  are primitive translation vectors of f.c.c. lattice.

We take into account the elements only on the same site and between nearest neighbor atomic sites. Therefore the transfer integral parameter is rewritten as

$$H_{nm} \equiv \sum_l e^{i\mathbf{k}\cdot\mathbf{R}_l} \int \phi_n^*(\mathbf{r}) \mathcal{H} \phi_m(\mathbf{r} - \mathbf{R}_l) d\mathbf{r} , \quad (8)$$

where the summation is taken over four nearest neighbors.

This approximation is valid in describing an valence band states of semiconductor because the valence electrons in semiconductor having covalent bonding are tightly bound to atomic sites, or in other words, the overlap of electronic wave functions between neighboring sites is considered to be very small.

In diamond and zinblende crystals, we obtain  $8 \times 8$  secular determinant [8]  $H_{nm}$  representing all possible nearest neighbor interactions as

$$\begin{bmatrix} E_{s_0} & V_{ss}g_0 & 0 & 0 & 0 & V_{s_0p}g_1 & V_{s_0p}g_2 & V_{s_0p}g_3 \\ V_{ss}g_0^* & E_{s_1} & -V_{s_1p}g_1^* & -V_{s_1p}g_2^* & -V_{s_1p}g_3^* & 0 & 0 & 0 \\ 0 & -V_{s_1p}g_1 & E_{p_0} & 0 & 0 & V_{xx}g_0 & V_{xy}g_3 & V_{xy}g_2 \\ 0 & -V_{s_1p}g_2 & 0 & E_{p_0} & 0 & V_{xy}g_3 & V_{xx}g_0 & V_{xy}g_1 \\ 0 & -V_{s_1p}g_3 & 0 & 0 & E_{p_0} & V_{xy}g_2 & V_{xy}g_1 & V_{xx}g_0 \\ V_{s_0p}g_1^* & 0 & V_{xx}g_0^* & V_{xy}g_3^* & V_{xy}g_2^* & E_{p_1} & 0 & 0 \\ V_{s_0p}g_2^* & 0 & V_{xy}g_3^* & V_{xx}g_0^* & V_{xy}g_1^* & 0 & E_{p_1} & 0 \\ V_{s_0p}g_3^* & 0 & V_{xy}g_2^* & V_{xy}g_1^* & V_{xx}g_0^* & 0 & 0 & E_{p_1} \end{bmatrix} \equiv H_{nm} , \quad (9)$$

where the function  $g_0$ ,  $g_1$ ,  $g_2$ , and  $g_3$  are given by

$$g_0(\mathbf{k}) = \cos \pi \frac{k_1}{2} \cos \pi \frac{k_2}{2} \cos \pi \frac{k_3}{2} - i \sin \pi \frac{k_1}{2} \sin \pi \frac{k_2}{2} \sin \pi \frac{k_3}{2} \quad (10)$$

$$g_1(\mathbf{k}) = -\cos \pi \frac{k_1}{2} \sin \pi \frac{k_2}{2} \sin \pi \frac{k_3}{2} + i \sin \pi \frac{k_1}{2} \cos \pi \frac{k_2}{2} \cos \pi \frac{k_3}{2} \quad (11)$$

$$g_2(\mathbf{k}) = -\sin \pi \frac{k_1}{2} \cos \pi \frac{k_2}{2} \sin \pi \frac{k_3}{2} + i \cos \pi \frac{k_1}{2} \sin \pi \frac{k_2}{2} \cos \pi \frac{k_3}{2} \quad (12)$$

$$g_3(\mathbf{k}) = -\sin \pi \frac{k_1}{2} \sin \pi \frac{k_2}{2} \cos \pi \frac{k_3}{2} + i \cos \pi \frac{k_1}{2} \cos \pi \frac{k_2}{2} \sin \pi \frac{k_3}{2} , \quad (13)$$

and

$$\mathbf{k} = \left( \frac{2\pi}{a} \right) (k_1, k_2, k_3) . \quad (14)$$

The parameters appearing in eq.(9) are given by eq.(8) where the alphabetical notations refer to the basis function of  $s$ - or  $p$ -orbital and the numeral notations

of "0" or "1" refer to the distinction between anion and cation. The parameters derived from two atomic orbitals depend on the atomic distance and on the direction cosines of the second atom with respect to the first atom.

Next, let us consider an overlap between atomic sites. While it is well known that the valence band is obtained successfully by tight-binding method using only the nearest neighbour transfer integral parameters, a poor fitting for the conduction band arises as the conventional difficulty of this method. In order to accomplish a better fitting to the conduction band as well as to the valence band, we introduce the following new set of parameters which are originated from the overlap integrals [10] of localized orbitals between the different atomic sites.

The overlap integral parameters are defined as

$$O_{n,m} \equiv \int \phi_n^*(\mathbf{r})\phi_m(\mathbf{r} - \mathbf{R}_l)dr \quad (15)$$

where the notations of  $n$ ,  $m$ , and  $\mathbf{R}_l$  are the same as those in the definition of the transfer integral parameters. Thus, the final eigenvalue problem to be solved is of the form

$$(H_{nm} - ES_{nm})\mathbf{\Lambda} = \mathbf{0} \quad , \quad (16)$$

where  $\mathbf{\Lambda}$  is column eigenvector,

$$S_{nm} \equiv \sum_l e^{i\mathbf{k}\cdot\mathbf{R}_l} \int \phi_n^*(\mathbf{r})\phi_m(\mathbf{r} - \mathbf{R}_l)dr \quad . \quad (17)$$

$S_{nm}$  is Hermitian matrix of  $8 \times 8$  and is represented similarly to the case of transfer integral parameters as eq.(9) except for that the diagonal matrix components are all equal to unity.

Consequently we have nine transfer integral parameters and five overlap integral parameters for zincblende structure, and also have seven transfer integral parameters and four overlap integral parameters for diamond structure, respectively.

### 3.2 Strain Dependence of Band Parameters

We determine the tight-binding parameters so as to reproduce the EPM results focusing on the high-symmetry points in the Brillouin zone, for example,  $X$ ,  $L$ ,

and  $\Gamma$ -point in the valence band. We later need the change in  $E_{bs}$  under the contraction or expansion. Thus strain dependence of tight-binding parameters have to be introduced. When the atomic distance is changed, we employ a  $d^{-2}$  dependence of the all band parameters, which is proposed by Harrison [9], where  $d$  is the nearest neighbour distance. For example,  $E'_{s0p}$  is given as

$$E'_{s0p} \equiv E_{s0p} \left( \frac{d_0}{d} \right)^2, \quad (18)$$

where  $d_0$  and  $d$  are atomic distances in an equilibrium state and in a distorted state, respectively. These parameters give a new band structure, new density of states, and consequently the variation of  $E_{bs}$  depending on lattice deformations.

### 3.3 Density of States

When we numerically calculate the density of states, we use a tetrahedron method [6]. First, we divide the Brillouin zone into a large number of tetrahedrons having equal volume [7], and make the assumption that the band dispersion is approximated to be linear inside each tetrahedron. Generally speaking, the density of states is represented as the number of allowed wave vector  $\mathbf{k}$  in the constant energy range from  $E$  to  $E+dE$ , Thus density of states  $N(E)$  is expressed as

$$N(E)dE = 2 \frac{\Omega}{2\pi} \int d\mathbf{k}, \quad (19)$$

where  $\Omega$  is volume of Brillouin zone. The integral for density of states is transformed into an integral over surface of constant energy. We arrive at the form

$$N(E) = \frac{2\Omega}{(2\pi)^3} \int_{E(\mathbf{k})=E} \frac{dS}{|\nabla_{\mathbf{k}} E|}, \quad (20)$$

which gives an explicit relation between the density of states and the band structure. This form is approximated by a sum over divided tetrahedrons.



$$N(E) \simeq \frac{2\Omega}{(2\pi)^3} \sum_{n,i} \frac{S_n(E, \mathbf{k}_i)}{|\nabla_{\mathbf{k}} E_n(\mathbf{k}_i)|} , \quad (21)$$

where  $n$  indicate band index,  $S_n(E, \mathbf{k}_i)$  is the surface area inside the  $i$ th tetrahedron, and  $\nabla_{\mathbf{k}} E_n(\mathbf{k}_i)$  is the  $\mathbf{k}$ -gradient at the tetrahedron center, i.e. the coefficient of the single first term Taylor-series expansion. In this scheme,  $\nabla_{\mathbf{k}} E_n(\mathbf{k}_i)$  are determined in terms of the corner energies and coordinates of the tetrahedron.

### 3.4 Results

We numerically calculated the eigenvalue equation of eq.(16) for the diamond and zincblende structures, Si, Ge, and GaAs, along  $\langle 1 1 1 \rangle$  and along  $\langle 0 0 1 \rangle$  which runs between the symmetry point  $\Gamma$ ,  $X$ ,  $L$ , and  $U$  of the Brillouin zone. These results of the energy band structures are shown in figs.3, 4, and 5 for above materials. Also, the sets of tight-binding parameters after the fitting to the EPM results are given in tables 1, 2, and 3, respectively. Nevertheless the improvement of the conduction band, the difficulty of fitting the conduction band is still remained.

## 4 Repulsive Force

### 4.1 Model

Now let us consider a short-range-force model as repulsive energy  $U$  which is defined as

$$U \equiv \sum_{i \neq j}^n A \exp(-\kappa |\mathbf{r}_i - \mathbf{r}_j|) , \quad (22)$$

where  $A$  and  $\kappa$  are parameters,  $|\mathbf{r}_i - \mathbf{r}_j|$  is the atomic distance between all atoms in the crystal. The value of repulsive energy decrease rapidly as the atomic distance is larger. Comparing with Si, the parameters  $A$  and  $\kappa$  in a compound semiconductor should be different between diferent pair of atoms, for example, GaAs, Ga-Ga, Ga-As, and As-As. However, for simplicity of calculation, we assume that the parameter values are same.

The parameters  $A$  and  $\kappa$  are determined semiempirically so as to satisfy the following two constraints.

$$\frac{\partial E_{tot}}{\partial V} = 0 \quad , \quad (23)$$

where  $V$  denotes volume. This condition means that  $E_{tot}$  should be minimum at equilibrium lattice constant. The second condition is that the curvature of local minimum of  $E_{tot}$  satisfies

$$V \frac{\partial^2 E_{tot}}{\partial V^2} = B \quad , \quad (24)$$

where  $B$  denotes the bulk modulus (in dyn/m<sup>2</sup>) of a specified semiconductor.

## 5 Results of Total Energy Calculations

### 5.1 $E_{tot}$ for Contraction and Expansion

The calculated variation of  $E_{bs}$  under the contraction or expansion for Si, Ge, and GaAs are shown in figs.6, 9, and 12, respectively. The width of variation for lattice constants of each case are taken within one percent of the equilibrium values. The overall dependencies of total energy on the distortion are all consistent with experimental results. The parameters  $A$  and  $\kappa$  are shown in figs.7, 10, and 13, respectively. The fitted results of bulk modulus  $B_{cal}$  (in dyn/m<sup>2</sup>) to the experimental values are shown in figs.8, 11, and 14, respectively. The number of calculated points for uniform deformations are five in this calculations. The results of calculations for  $E_{bs}$  and  $E_{tot}$  are interperated by the least error fitting with the third order polynominals. In order to obtain the sufficiently smooth fitting with respect to the variation of  $E_{tot}$  as a function of atomic distance, the necessary accuracy for the integration with respect to the density of states is about 10<sup>-4</sup> orders. The results of these calculations are plotted with different scale.

### 5.2 $E_{tot}$ for Uniaxial Strain

Now, let us investigate the case that a  $\langle 100 \rangle$  uniaxially stress is applied, typically, as in a strained layered superlattice. When a stress is applied to a crystalline

material, some distortion would arise inside. Of course, total energy should be increased under such stress.

Specifically, we investigate the case that the tetragonal deformation is introduced in the crystal. Here the strains, i.e.  $(a/a_0 - 1) \times 100$  are assumed only  $\pm 1\%$  where  $a_0$  is an equilibrium lattice constant. In addition we impose a condition that the volume is kept constant even under the existence of a strain. Therefore lattice constant  $c$  of the tetragonal lattice is determined as  $c = a_0^3/a^2$ . It greatly simplifies the tetrahedrally strained bonding shapes. A 1/8 of the primitive cell having lattice constant  $a_0$  is depicted schematically in fig.15. In this sense, the tight-binding parameters depend only on the change of the bond length  $d$  and on the directional cosines of the bonding atoms.

Necessarily, the shape of the Brillouin zone under a  $\langle 100 \rangle$  uniaxial stress is deformed. Schematic illustrations corresponding to the above each strained primitive cell (see fig.15) are shown in fig.16. The high symmetry points of the Brillouin zone are also shown in which the name of the high symmetry points are different from the case shown in fig.2. The numerical computations are carried out by the same method as the case of contraction or expansion and give us results of variation as a function of strain. The parameters  $A$  and  $\kappa$  are fixed on each fitting result.

## 6 Discussion

The numerically calculated number of valence electrons obtained by integrating the density of states, which must be four, gave a slightly different value. The accuracy is about  $10^{-4}$  orders including the computational error of the area integral. In order to improve the accuracy of the calculations, we should divide the Brillouin zone into much smaller tetrahedrons or should take smaller dividing of the energy region with respect to the numerical integration over the valence band, while we here divided the Brillouin zone into about 100,000 pieces and divided the energy region into about 1,000 elements.

In the case of uniform contraction or expansion,  $E_{bs}$  which is one of the factors of  $E_{tot}$ , monotonously varied depending on the atomic distance. It is quite plausible because we have employed the  $d^{-2}$ -dependence on the tight-binding parameters. Namely when the atomic distance become smaller, the valence band would be wider, and the integral in eq.(4) would contribute to the much lower energy of the valence band. As a result of this effect,  $E_{bs}$  would decrease.

On the contrary to  $E_{bs}$ ,  $U$  monotonously increased when the atomic distance become smaller. The curvatures of  $U$  greatly contributed to the bulk modulus calculations for the calculated result of total energy and were determined by parameter fitting of  $A$  and  $\kappa$ . For Si, we were not be able to choose the parameter which gives the result of the experiment and the fitting was at most about one order of magnitude smaller than the experimental value. For Ge and GaAs, it is possible to fit to the experimental bulk modulus by the certain choice of parameters.

From the experimental data of the thermal expansion coefficient, the crystal expands only about a few  $10^{-3}\%$ . Without the great improvements of the accuracy in the  $E_{bs}$  calculation about  $10^{-6}$  orders, we can not discuss the thermal effect. The difficulty in the improvement of accuracy is in the integration of the density of states which has quite complicated fine structures reflecting the band structures. Also the computational difficulty of calculating the density of states including 'flat band' appearing in the band structure.

In the investigation under the existence of a  $\langle 100 \rangle$  uniaxial stress, the variations of  $U$  indicates two local minimum under the two tetragonal deformations which are both a few percent displaced from the equilibrium shape. The double minimum does not appear when the value of parameter  $\kappa$  less than about 5 in the unit of inverse of lattice constant. In our fitting to the experimental elastic properes, we always obtained the value of  $\kappa$  greater than 5. If we assumed  $U$  to be a more short-range-force type, the double minimum will appear more apparently. A qualitative reason for this particuler property can be interpreted

as follows. The diamond and zincblende structures are not stable with respect to the ioncore repulsive force but stabilized with including the electronic contribution from covalently bonded valence electrons. Actually in our calculation, the double minimum of  $U$  disappeared from the results of  $E_{tot}$  because the contribution of  $E_{bs}$  becomes dominant for determining  $E_{tot}$ . In this sense,  $E_{tot}$  has minimum at the equilibrium atomic configuration.

## 7 Concluding Remarks

We proposed a simple method and treatment to evaluate the structural stabilities for the group IV and the group III-V semiconductors. The correspondence to the experimental results is well except Si for which we were not able to reach the consistent results with respect to fitting to the bulk modulus. In the case of a  $\langle 100 \rangle$  uniaxial strain, we need more detailed investigations about the results that the repulsive energies have double minimum tendencies and about the validity of the repulsive potential assumed to be of exponential form. In order to apply this simple method to the structural stabilities of superlattices, we should improve the computational accuracy of the band structure energy calculation. The approximation that parameters,  $A$  and  $\kappa$ , included in the repulsive potential are same should be improved for compound semiconductors. Finally, our method would be useful to evaluate stable structure for hypothetically designed artificial materials in a relatively simple way comparing *ab initio* calculation.

## References

- [1] *Handbook on Semiconductors Materials, Properties and Preparation*, Vol.3, edited by T. S. Moss, (North-Holland Publishing Company, 1981), chap.9.
- [2] J. C. Slater and G. F. Koster, *Phys. Rev.* 94, 1498 (1954).
- [3] M. L. Cohen and J. R. Chelikowsky, *Electronic Structure and Optical Properties of Semiconductors*, edited by M. Cardona, (Springer-Verlag, 1988), chaps.3 and 8.
- [4] N. W. Achcroft and N. D. Mermin, *Solid State Physics*, (W. B. Saunders Company, 1976), chaps.4, 5 and 10.
- [5] D. J. Chadi, *Phys. Rev. B* 19, 2074 (1979).
- [6] J. Rath and A. J. Freeman, *Phys. Rev. B* 11, 2109 (1975).
- [7] W. A. Harrison, *Electronic Structure and the Properties of Solid, The Physics of the Chemical Bond*, (1980), chap.2.
- [8] D. J. Chadi and M. L. Cohen, *Phys. Stat. Sol. (b)* 68, 405 (1975).
- [9] W. A. Harrison, *J. Vac. Sci. Technol.*, 14, 1016 (1977).
- [10] D. J. Chadi, *Phys. Rev. B* 16, 3572 (1977).

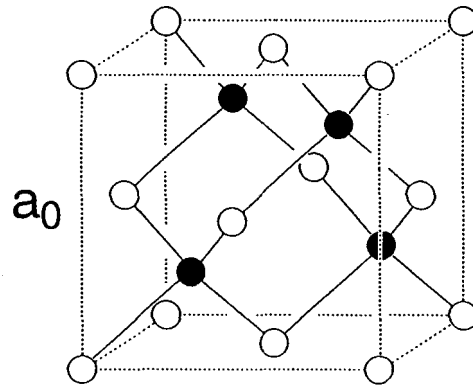


**Fig.1** : Zincblende structure including the regular tetrahedrally bonded atoms with four nearest neighbors. In the diamond structure both the shaded and unshaded sites are occupied by same kinds of atoms.

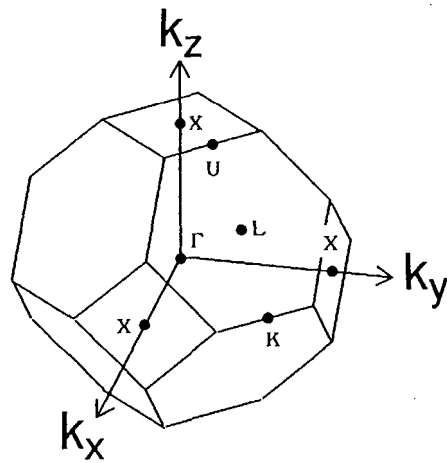


**Fig.2** : First Brillouin zone of the diamond or zincblende structure, which is the primitive cell of  $k$ -space. The high symmetry points are named  $\Gamma$  ( $k=0$ ),  $X$ ,  $K$ ,  $U$ , and  $W$ .

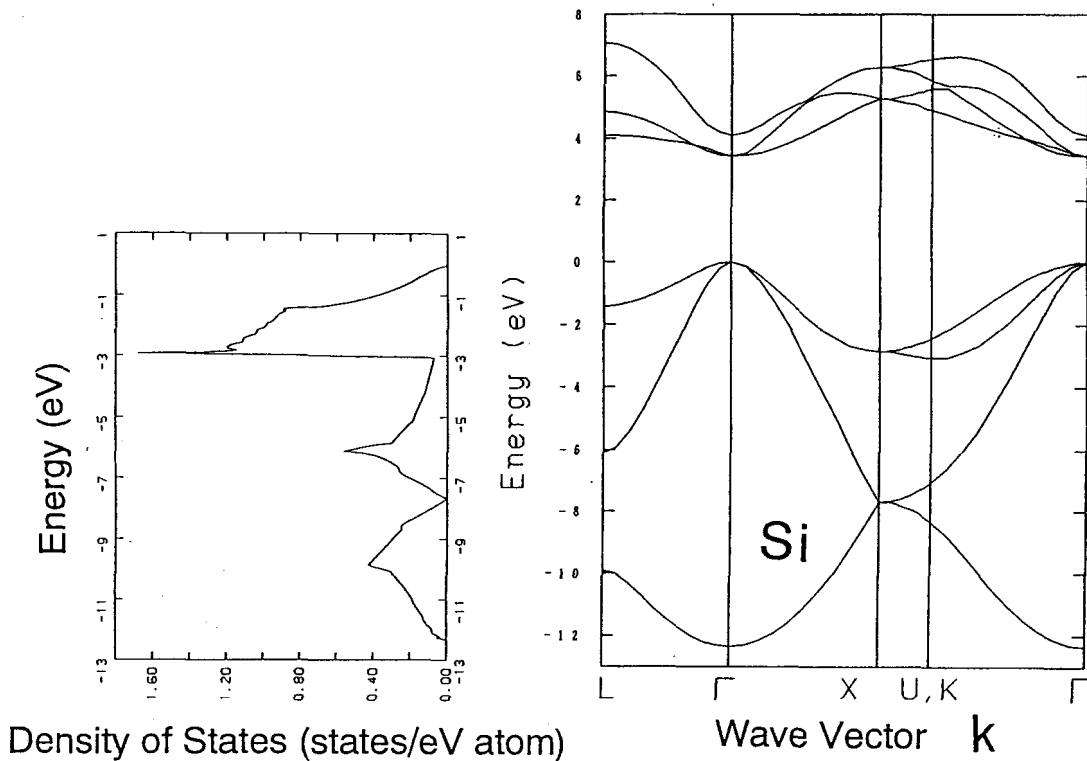


Fig.3 : Energy band structure of Si obtained by calculations by means of the tight-binding method. And the density of states of Si obtained by tight-binding parameters for the nearest neighbors interactions.

$E_{s0}$	$E_{s1}$	$E_{p0}$	$E_{p1}$	$V_{ss}$	$V_{s0p}$	$V_{s1p}$	$V_{xx}$	$V_{xy}$
0.0	0.0	5.840	5.840	-8.230	5.785	5.785	1.710	4.570

$O_{ss}$	$O_{s0p}$	$O_{s1p}$	$O_{xx}$	$O_{xy}$
0.0	0.0	0.0	0.0	0.0

Table 1 : Tight-binding parameters (in eV) of Si.



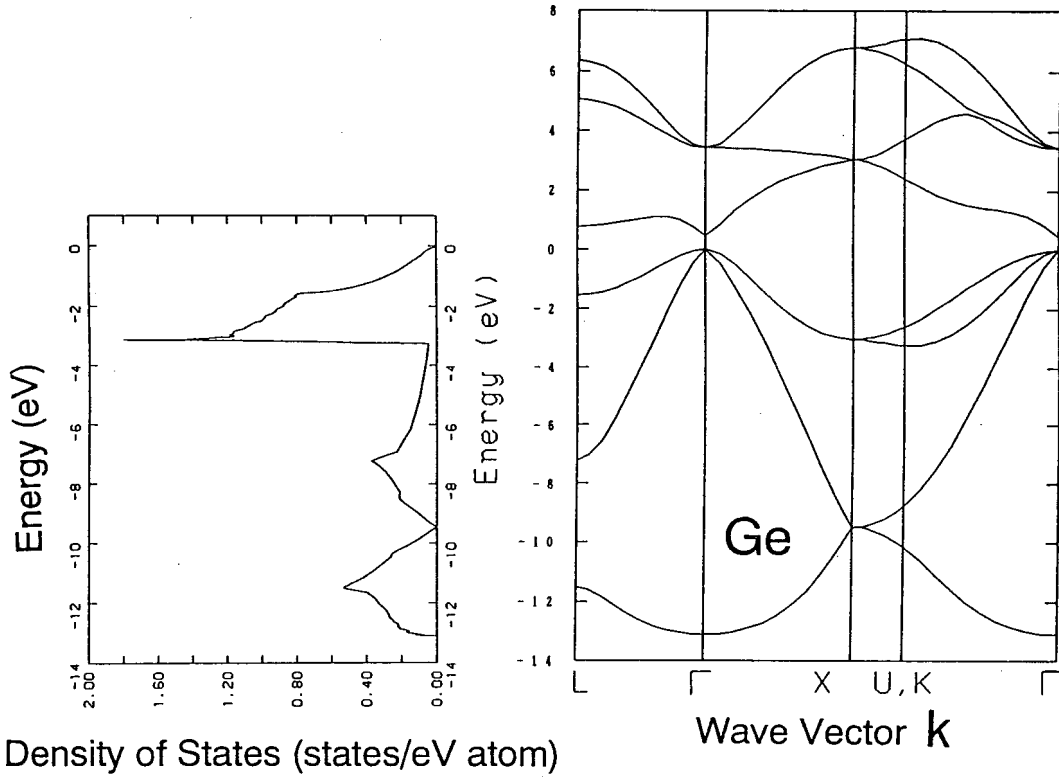


Fig.4 : Energy band structure of Ge obtained by calculations by means of the tight-binding method. And the density of states of Ge obtained by tight-binding parameters for the nearest neighbors interactions.

$E_{s0}$	$E_{s1}$	$E_{p0}$	$E_{p1}$	$V_{ss}$	$V_{s0p}$	$V_{s1p}$	$V_{xx}$	$V_{xy}$
-10.711	-10.711	-2.4985	-2.4985	-7.0061	3.2650	3.2650	1.6425	4.9668

$O_{ss}$	$O_{s0p}$	$O_{s1p}$	$O_{xx}$	$O_{xy}$
0.0201	0.1849	0.1849	0.0235	-0.0254

Table 2 : Tight-binding parameters (in eV) of Ge.

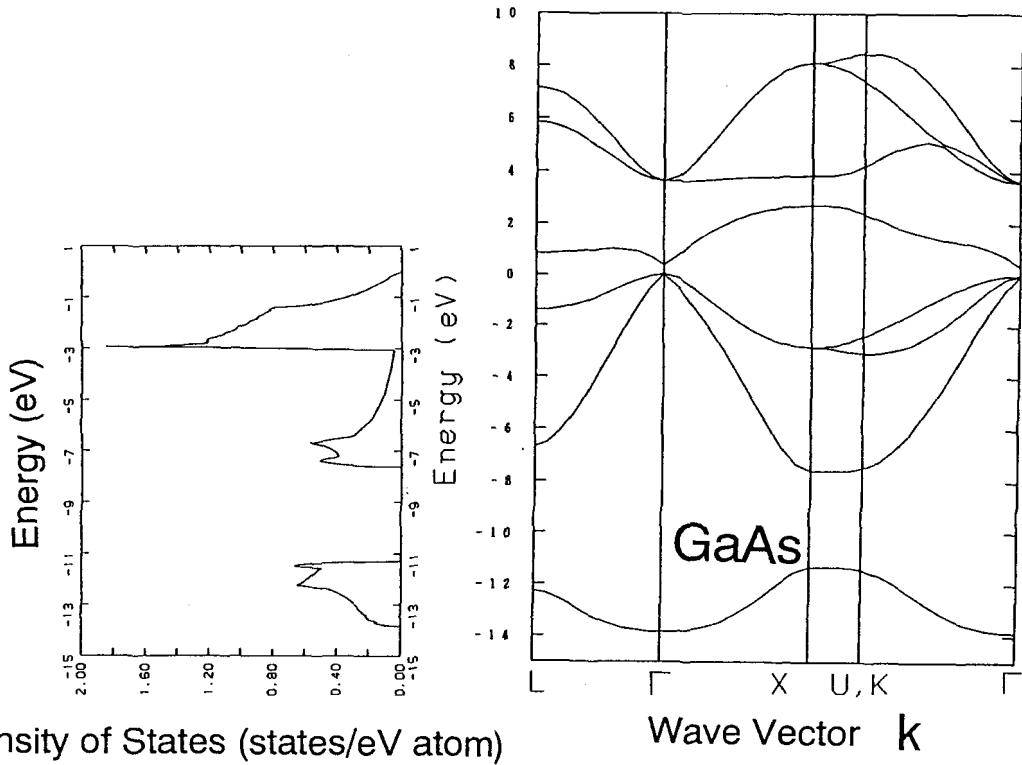
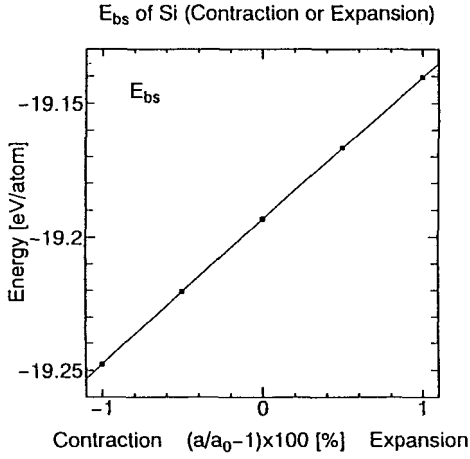


Fig.5 : Energy band structure of GaAs obtained by calculations by means of the tight-binding method. And the density of states of GaAs obtained by tight-binding parameters for the nearest neighbors interactions.

$E_{s0}$	$E_{s1}$	$E_{p0}$	$E_{p1}$	$V_{ss}$	$V_{s0p}$	$V_{s1p}$	$V_{xx}$	$V_{xy}$
-10.887	-6.5740	0.3634	-0.9936	-7.0553	4.8090	4.0933	1.6560	5.2373

$O_{ss}$	$O_{s0p}$	$O_{s1p}$	$O_{xx}$	$O_{xy}$
0.0337	0.0239	0.1194	-0.2207	-0.2207

Table 3 : Tight-binding parameters (in eV) of GaAs.



**Fig.6 :** The band structure energy  $E_{bs}$  of Si by using the tight-binding parameters. It correspond to attractive energy.

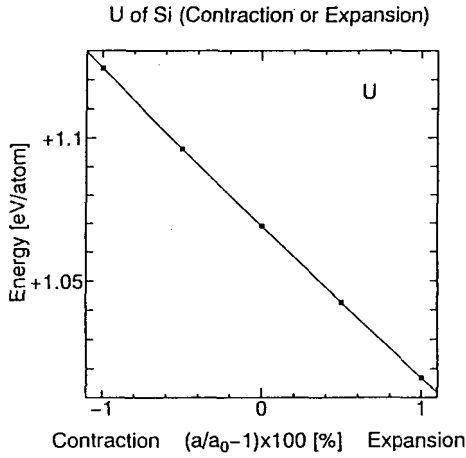


**Fig.7 :** The repulsive energy  $U$  of Si by using the exponential type model included two parameters  $A$  and  $\kappa$ . Fitting results of  $A=32.0$  and  $\kappa=10.0$ .

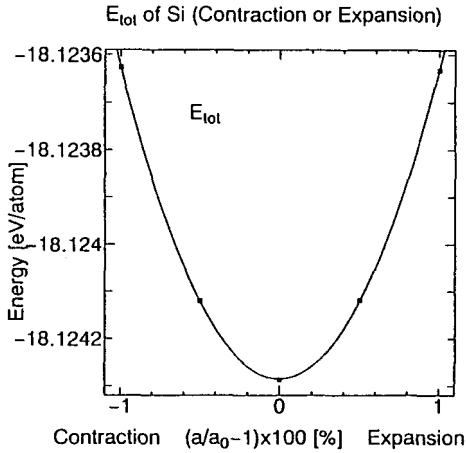


**Fig.8 :** The total energy  $E_{tot}$  of Si derived from the sum  $E_{bs}$  and  $U$ .  $E_{tot}$  is minimum at  $a/a_0 =$  unity. Bulk modulus  $B_{cal}$  is compared with experimental value  $B_{ex}$  (dyn/m<sup>2</sup>).  
 $B_{cal}/B_{ex} = 0.1215$

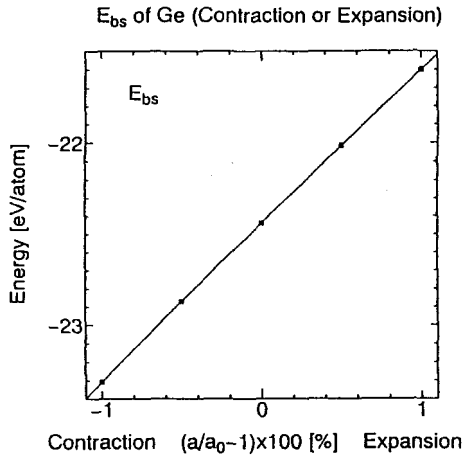


**Fig.9 :** The band structure energy  $E_{bs}$  of Ge by using the tight-binding parameters. It correspond to attractive energy.

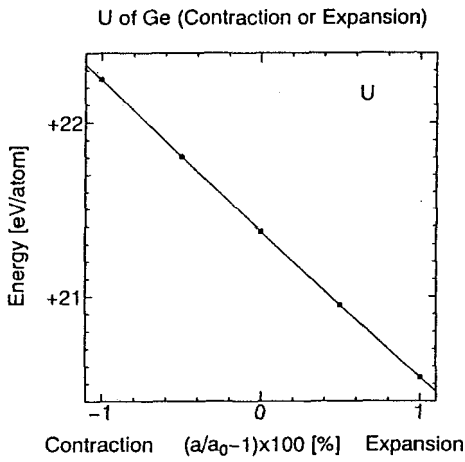


**Fig.10 :** The repulsive energy  $U$  of Ge by using the exponential type model included two parameters  $A$  and  $\kappa$ . Fitting results of  $A=80.92$  and  $\kappa=6.2861$ .

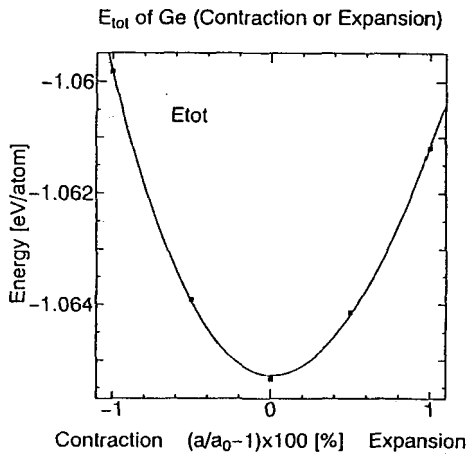


**Fig.11 :** The total energy  $E_{tot}$  of Ge derived from the sum  $E_{bs}$  and  $U$ .  $E_{tot}$  is minimum at  $a/a_0 =$  unity. Bulk modulus  $B_{cal}$  is compared with experimental value  $B_{ex}$  ( $\text{dyn}/\text{m}^2$ ).  
 $B_{cal}/B_{ex} = 1.000$

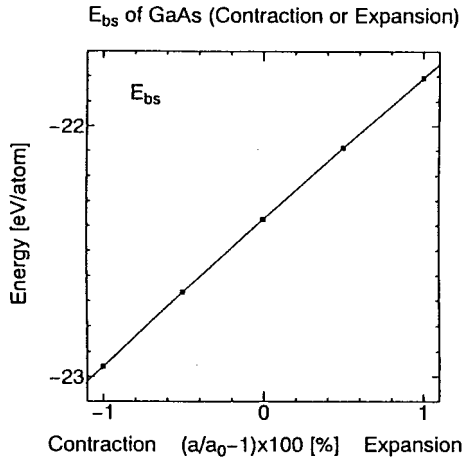


**Fig.12** : The band structure energy  $E_{bs}$  of GaAs by using the tight-binding parameters. It correspond to attractive energy.

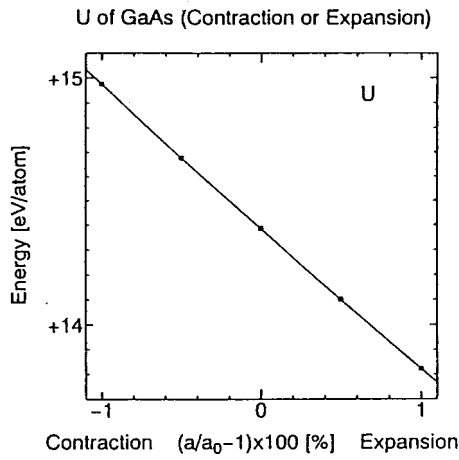


**Fig.13** : The repulsive energy  $U$  of GaAs by using the exponential type model included two parameters  $A$  and  $\kappa$ . Fitting results of  $A=54.915$  and  $\kappa=6.2991$ .

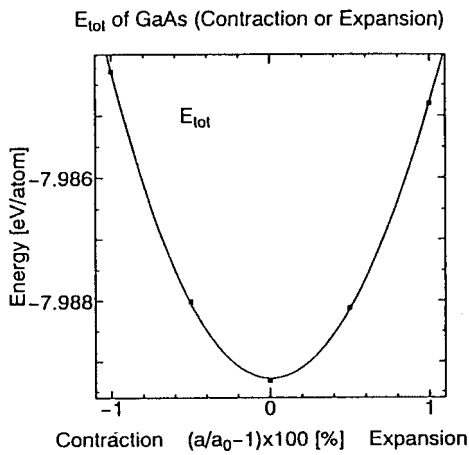


**Fig.14** : The total energy  $E_{tot}$  of GaAs derived from the sum  $E_{bs}$  and  $U$ .  $E_{tot}$  is minimum at  $a/a_0 = \text{unity}$ . Bulk modulus  $B_{cal}$  is compared with experimental value  $B_{ex}$  (dyn/m<sup>2</sup>).  
 $B_{cal}/B_{ex} = 1.000$

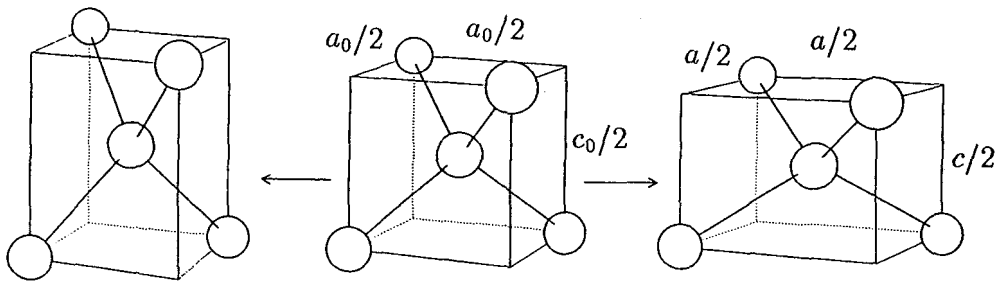


**Fig.15 :** The "pole-like" primitive cell with  $a < a_0$ ,  $c = a_0^3/a^2$  and the "plate-like" primitive cell with  $a > a_0$ ,  $c = a_0^3/a^2$  are shown in left hand and right hand of the series of figures. In strained cell the covalent bonding is also strained and the bond length is not same as the case of equilibrium lattice shown in center of the series of figures.

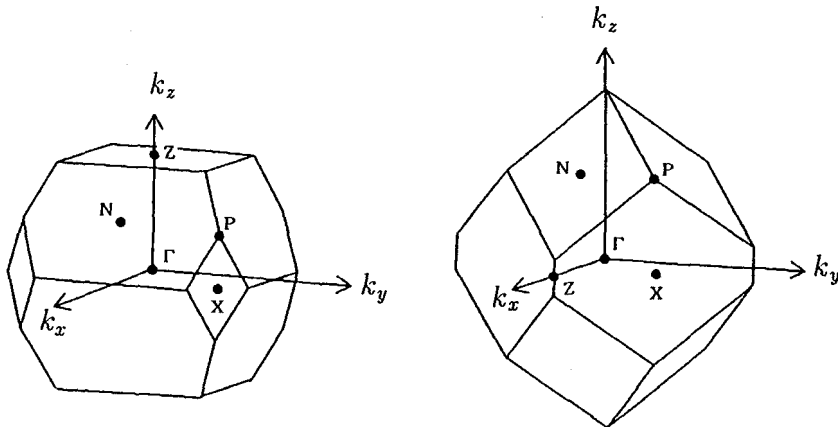


**Fig.16 :** Deformed Brillouin zone influenced in a (100) uniaxial stress. The alphabetical notations express high symmetry points  $\Gamma$ ,  $N$ ,  $P$ ,  $Z$ , and  $X$  differ from the case of equilibrium Brillouin zone(see fig.2).

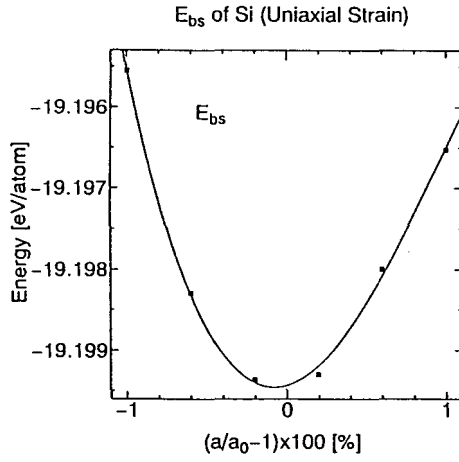


Fig.17 : The band structure energy  $E_{bs}$  of Si for a (100) uniaxial strain. The tight-binding parameters in Table 1 are used. It correspond to attractive energy.

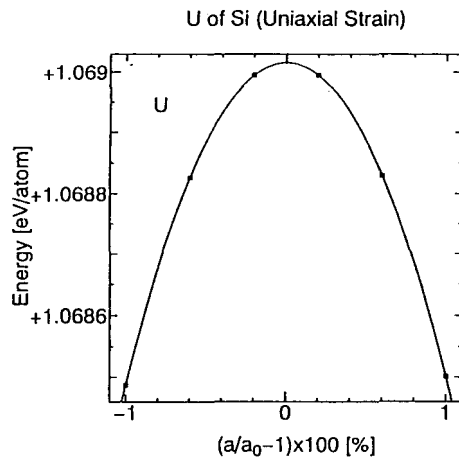


Fig.18 : The repulsive energy  $U$  of Si for a (100) uniaxial strain. The exponential form as an assumption of the repulsive energy is included two parameters  $A$  and  $\kappa$ . Fitting results of  $A$  and  $\kappa$  are used.

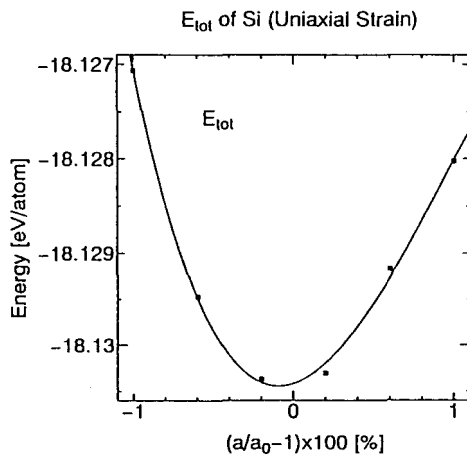
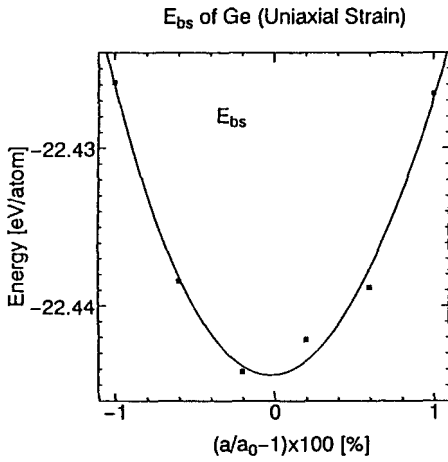
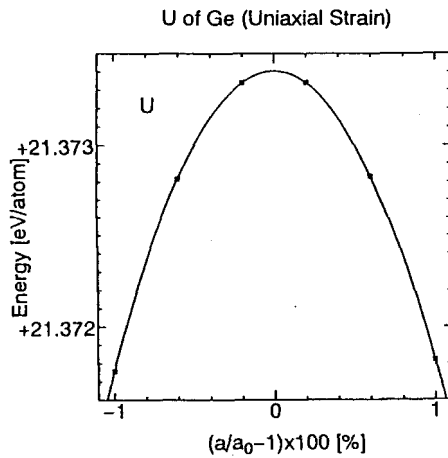


Fig.19 : The total energy  $E_{tot}$  of Si for a (100) uniaxial strain are derived from the sum  $E_{bs}$  and  $U$ .  $E_{tot}$  is minimum at  $a/a_0 =$  unity.



**Fig.20** : The band structure energy  $E_{bs}$  of Ge for a (100) uniaxial strain. The tight-binding parameters in Table 2 are used. It correspond to attractive energy.



**Fig.21** : The repulsive energy  $U$  of Ge for a (100) uniaxial strain. The exponential form as an assumption of the repulsive energy is included two parameters  $A$  and  $\kappa$ . Fitting results of  $A$  and  $\kappa$  are used.

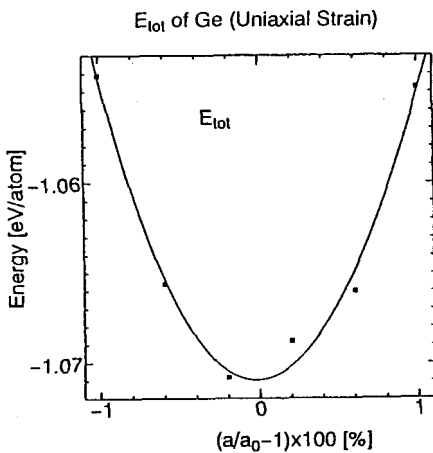


**Fig.22** : The total energy  $E_{tot}$  of Ge for a (100) uniaxial strain are derived from the sum  $E_{bs}$  and  $U$ .  $E_{tot}$  is minimum at  $a/a_0 =$  unity.

$$B = 0.256 \times 10^{13} (\text{dyn}/\text{m}^2).$$



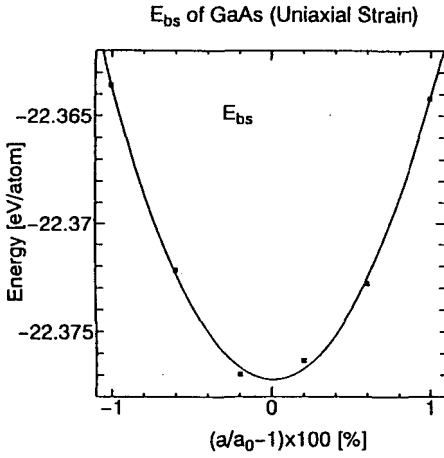


**Fig.23 :** The band structure energy  $E_{bs}$ , of GaAs for a (100) uniaxial strain. The tight-binding parameters in Table 3 are used. It correspond to attractive energy.

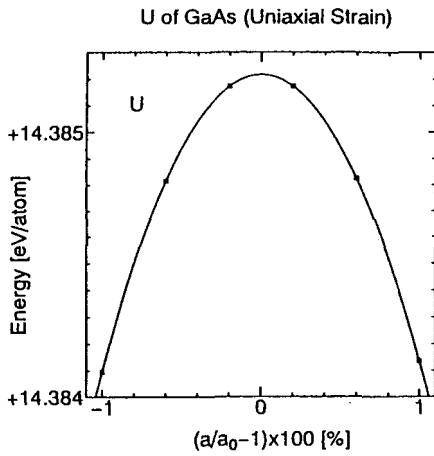


**Fig.24 :** The repulsive energy  $U$  of GaAs for a (100) uniaxial strain. The exponential form as an assumption of the repulsive energy is included two parameters  $A$  and  $\kappa$ . Fitting results of  $A$  and  $\kappa$  are used.

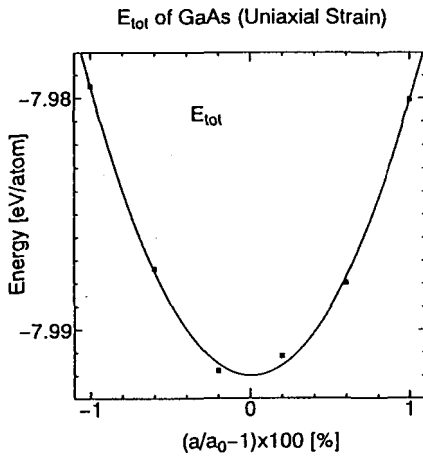


**Fig.25 :** The total energy  $E_{tot}$  of GaAs for a (100) uniaxial strain are derived from the sum  $E_{bs}$ , and  $U$ .  $E_{tot}$  is minimum at  $a/a_0 =$  unity.

$B = 0.192 \times 10^{13}(\text{dyn}/\text{m}^2).$